

Sequential Reduction of High Hydride Count Octahedral Rhodium Clusters $[\text{Rh}_6(\text{PR}_3)_6\text{H}_{12}][\text{BAR}^{\text{F}}_4]_2$: Redox-Switchable Hydrogen Storage

Simon K. Brayshaw,[†] Andrew Harrison,^{‡,§} J. Scott McIndoe,^{||} Frank Marken,[†]
Paul R. Raithby,[†] John E. Warren,[⊥] and Andrew S. Weller^{*,†}

Contribution from the Department of Chemistry, University of Bath, BA2 7AY, U.K., Institut Laue-Langevin, 6, rue Jules Horowitz, BP 156 - 38042 Grenoble, Cedex 9, France, School of Chemistry and EaStChem, The University of Edinburgh, The King's Buildings, Edinburgh, EH9 3JJ, U.K., Department of Chemistry, University of Victoria, Victoria, BC V8W3V6, Canada, and CCLRC Daresbury Laboratory, Daresbury, Warrington, WA4 4AD, U.K.

Received September 27, 2006; E-mail: a.s.weller@bath.ac.uk

Abstract: Cyclic voltammetry on the octahedral rhodium clusters with 12 bridging hydride ligands, $[\text{Rh}_6(\text{PR}_3)_6\text{H}_{12}][\text{BAR}^{\text{F}}_4]_2$ ($\text{R} = \text{Cy}$ **Cy-[H12]**²⁺, $\text{R} = \text{Pr}$ **Pr-[H12]**²⁺; $[\text{BAR}^{\text{F}}_4]^- = [\text{B}\{\text{C}_6\text{H}_3(\text{CF}_3)_2\}_4]^-$) reveals four potentially accessible redox states: $[\text{Rh}_6(\text{PR}_3)_6\text{H}_{12}]^{0/1+2+/3+}$. Chemical oxidation did not produce stable species, but reduction of **Cy-[H12]**²⁺ using $\text{Cr}(\eta^6\text{-C}_6\text{H}_6)_2$ resulted in the isolation of **Cy-[H12]**⁺. X-ray crystallography and electrospray mass spectrometry (ESI-MS) show this to be a monocation, while EPR and NMR measurements confirm that it is a monoradical, $S = 1/2$, species. Consideration of the electron population of the frontier molecular orbitals is fully consistent with this assignment. A further reduction is mediated by $\text{Co}(\eta^5\text{-C}_5\text{H}_5)_2$. In this case the cleanest reduction was observed with the tri-isopropyl phosphine cluster, to afford neutral **Pr-[H12]**. X-ray crystallography confirms this to be neutral, while NMR and magnetic measurements (SQUID) indicate an $S = 1$ paramagnetic ground state. The clusters **Cy-[H12]**⁺ and **Pr-[H12]** both take up H_2 to afford **Cy-[H14]**⁺ and **Pr-[H14]**, respectively, which have been characterized by ESI-MS, NMR spectroscopy, and UV-vis spectroscopy. Inspection of the frontier molecular orbitals of $S = 1$ **Pr-[H12]** suggest that addition of H_2 should form a diamagnetic species, and this is the case. The possibility of "spin blocking" in this H_2 uptake is also discussed. Electrochemical investigations on the previously reported **Cy-[H16]**²⁺ [*J. Am. Chem. Soc.* **2006**, *128*, 6247] show an irreversible loss of H_2 on reduction, presumably from an unstable **Cy-[H16]**⁺ species. This then forms **Cy-[H12]**²⁺ on oxidation which can be recharged with H_2 to form **Cy-[H16]**²⁺. We show that this loss of H_2 is kinetically fast (on the millisecond time scale). Loss of H_2 upon reduction has also been followed using chemical reductants and ESI-MS. This facile, reusable gain and loss of 2 equiv of H_2 using a simple one-electron redox switch represents a new method of hydrogen storage. Although the overall storage capacity is very low (0.1%) the attractive conditions of room temperature and pressure, actuation by the addition of a single electron, and rapid desorption kinetics make this process of interest for future H_2 storage applications.

Transition metal clusters offer unique perspectives in molecular chemistry: They represent soluble molecular models for metal particles, are generally of high symmetry, have delocalized electronic structures, and have narrowly spaced frontier molecular orbitals which also show a high degree of metal character, while the core metal structure is often characterized by structural integrity. All these facets lead to a significant interest in the redox chemistry and magnetism of transition metal clusters, and many support sequential redox events and show paramagnetism in isolated species.^{1–4} For the later transition

metal clusters with π -accepting ligands, typically carbon monoxide, multiple redox steps have been observed, and up to 10 sequential reversible reductions have been reported for the high-nuclearity platinum cluster $[\text{Pt}_{26}(\text{CO})_{32}]^n$ ($n = 0$ to -10).⁵ Indeed such condensed metal carbonyl clusters have been termed "electron sinks"⁶ and often display rich electrochemistry associated with the reversible addition of electrons. Given this, only a handful of late-transition metal clusters with π -accepting ligands have been reported in which chemically reversible redox pairs can be isolated and characterized spectroscopically,⁶ or

[†] University of Bath.

[‡] Institut Laue-Langevin.

[§] The University of Edinburgh.

^{||} University of Victoria.

[⊥] CCLRC Daresbury Laboratory.

(1) Lemoine, P. *Coord. Chem. Rev.* **1982**, *47*, 55–88.

(2) Geiger, W. E.; Connelly, N. G. *Adv. Organomet. Chem.* **1985**, *24*, 87–130.

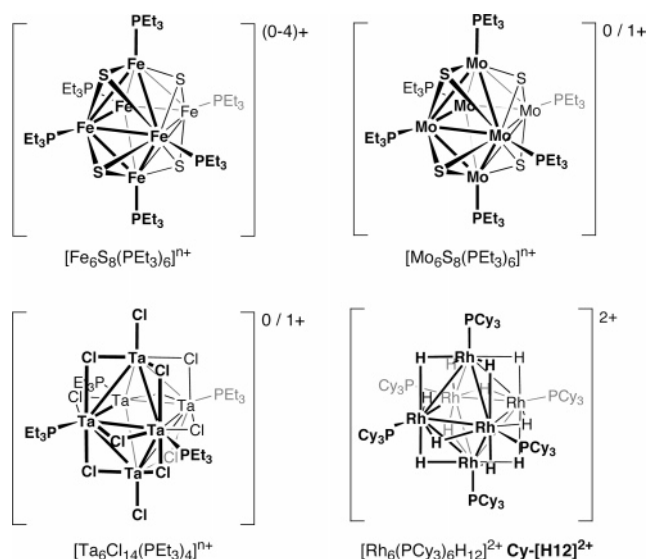
(3) Zanello, P. *Struct. Bonding* **1992**, *79*, 101–214.

(4) Zanello, P. *Inorganic Electrochemistry*; Royal Society of Chemistry: Cambridge, 2003.

(5) Roth, J. D.; Lewis, G. J.; Safford, L. K.; Jiang, X. D.; Dahl, L. F.; Weaver, M. J. *J. Am. Chem. Soc.* **1992**, *114*, 6159–6169.

(6) Longoni, G.; Femoni, C.; Iapalucci, M. C.; Zanello, P. In *Metal Clusters in Chemistry*; Braunstein, P., Oro, L. A., Raithby, P. R., Eds.; Wiley-VCH: Weinheim, 1999; Vol. 2.

Scheme 1



even more rarely crystallographically.^{4,7–10} In contrast, different redox states of transition metal clusters with π -donating ligands (such as chalcogens and halides) are often synthetically more accessible, and crystallographic characterization of three members of the trigonal prismatic clusters $[W_6CCl_{18}]^{n-}$ ($n = 0$ to 4)¹¹ and $[W_6NCl_{18}]^{n-}$ ($n = 1$ to 3),¹² four of $[Fe_6S_8(PEt_3)_6]^{n+}$ ($n = 0$ to 4),¹³ and two of $[Mo_6S_8(PEt_3)_6]^{n+}$ ($n = 1+$ to 2–)¹⁴ have been described, among others.⁴ Hexanuclear cluster compounds with edge-bridged halide ligands also exhibit extensive redox behavior,^{15–17} and redox pairs such as $[Ta_6Cl_{14}(PEt_3)_4]^{n+}$ ($n = 0, 1$)¹⁸ have been structurally characterized (Scheme 1). The redox flexibility apparent in many of these clusters comes from the ease of addition or removal of electrons from metal-localized orbitals (Figure 1).

We have recently reported the synthesis of a new class of transition metal cluster, $[Rh_6(PR_3)_6H_{12}][BAR^F_4]_2$ ($R = Cy$ **Cy-[H12]**²⁺, ^{Pr}**Pr-[H12]**²⁺; $[BAR^F_4]^- = [B\{C_6H_3(CF_3)_2\}_4]^-$) which are composed of late transition metal centers (Rh) but have structures that are directly analogous to early transition metal clusters with edge-bridged halide ligands, such as $[Nb_6Cl_{18}]^{4-}$, in that each Rh–Rh edge in the octahedron is bridged by a hydride ligand (Scheme 1).^{19,20} This similarity extends to the

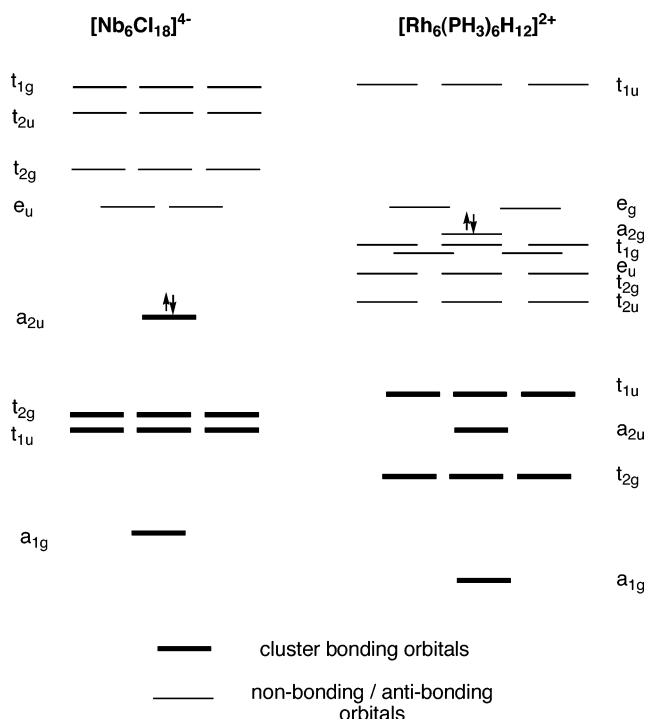


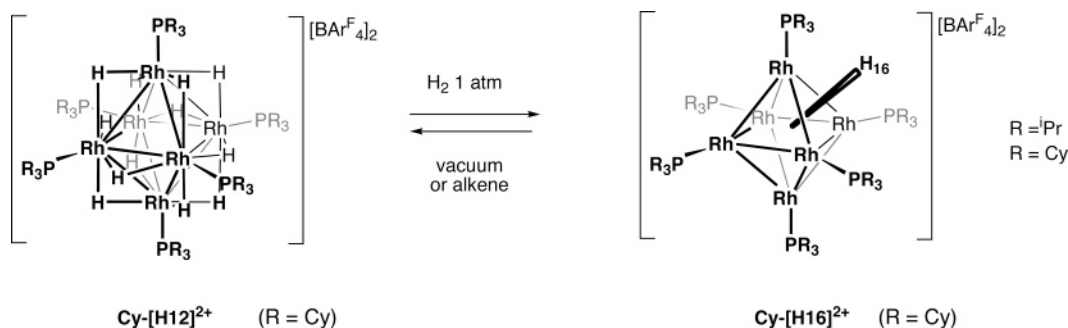
Figure 1. Comparative energy level diagram for $[Nb_6Cl_{18}]^{4-}$ and $[Rh_6(PR_3)_6H_{12}]^{2+}$ constrained to O_h symmetry.^{20–22} Only metal–metal localized orbital interactions are shown. The diagram is intended to outline the pattern and occupancy of these orbitals, and comparisons of the relative energies of particular orbitals between cluster species should be taken only as approximate.

electronic structure of the rhodium clusters, which show eight orbitals involved in metal–metal bonding which are of the same symmetry as those of the halide-bridged clusters.^{21,22} However, the move from group 5 metals (e.g., Nb) with bridging halides to a group 9 metal (Rh) with phosphines and hydrides results in 12 additional metal-localized filled orbitals primarily of nonbonding nature in $[Rh_6(PR_3)_6H_{12}][BAR^F_4]_2$.

Calculations also show that under octahedral symmetry $[Rh_6(PR_3)_6H_{12}][BAR^F_4]_2$ (generically referred to as **[H12]**²⁺) has two, low lying, empty orbitals of e_g symmetry, only ~ 0.3 eV higher in energy than the a_{2g} HOMO. These orbitals are well set up to receive four electrons, and we have demonstrated this by the facile addition of two molecules of H_2 to afford $[Rh_6(PR_3)_6H_{16}][BAR^F_4]_2$ **[H16]**²⁺ (Scheme 2).^{20,23} This results in an electronic configuration that shows a significantly larger HOMO–LUMO gap (1.3 eV). A similar set of low-lying orbitals in the unsaturated cluster $Pt_3Re_2(CO)_6(P^tBu_3)_3$ also allow the uptake of H_2 , in this case 3 equiv per cluster.²⁴ For $[Rh_6(PR_3)_6H_{16}][BAR^F_4]_2$, H_2 addition is reversible (and can be cycled), as placing under a vacuum (5×10^{-3} Torr) or addition of a hydrogen acceptor such as *tert*-butylethene (tbe) regenerates $[Rh_6(PR_3)_6H_{12}][BAR^F_4]_2$, **[H12]**²⁺, quantitatively.^{20,23} The PCy_3 functionalized cluster (**Cy-[H12]**²⁺) holds onto the hydrogen much more strongly than the ⁱPr₃ cluster (days versus hours, respectively, when placed under a vacuum). We attribute this

- (7) Paquette, M. S.; Dahl, L. F. *J. Am. Chem. Soc.* **1980**, *102*, 6621–6623.
 (8) Longoni, G.; Manassero, M.; Sansoni, M. *J. Am. Chem. Soc.* **1980**, *102*, 7973–7974.
 (9) Albright, T. A.; Yee, K. A.; Saillard, J. Y.; Kahlal, S.; Halet, J. F.; Leigh, J. S.; Whitmire, K. H. *Inorg. Chem.* **1991**, *30*, 1179–1190.
 (10) Ragaini, F.; Ramage, D. L.; Song, J. S.; Geoffroy, G. L.; Rheingold, A. L. *J. Am. Chem. Soc.* **1993**, *115*, 12183–12184.
 (11) Welch, E. J.; Crawford, N. R. M.; Bergman, R. G.; Long, J. R. *J. Am. Chem. Soc.* **2003**, *125*, 11464–11465.
 (12) Welch, E. J.; Yu, C. L.; Crawford, N. R. M.; Long, J. R. *Angew. Chem., Int. Ed.* **2005**, *44*, 2549–2553.
 (13) Goddard, C. A.; Long, J. R.; Holm, R. H. *Inorg. Chem.* **1996**, *35*, 4347–4354.
 (14) Saito, T.; Yamamoto, N.; Nagase, T.; Tsuboi, T.; Kobayashi, K.; Yamagata, T.; Imoto, H.; Unoura, K. *Inorg. Chem.* **1990**, *29*, 764–770.
 (15) Prokopuk, N.; Shriver, D. F. In *Advances in Inorganic Chemistry*; 1999; Vol. 46, pp 1–49.
 (16) Prokopuk, N.; Kennedy, V. O.; Stern, C. L.; Shriver, D. F. *Inorg. Chem.* **1998**, *37*, 5001–5006.
 (17) Klendworth, D. D.; Walton, R. A. *Inorg. Chem.* **1981**, *20*, 1151–1155.
 (18) Imoto, H.; Hayakawa, S.; Morita, N.; Saito, T. *Inorg. Chem.* **1990**, *29*, 2007–2014.
 (19) Ingleson, M. J.; Mahon, M. F.; Raithby, P. R.; Weller, A. S. *J. Am. Chem. Soc.* **2004**, *126*, 4784–4785.
 (20) Brayshaw, S. K.; Ingleson, M. J.; Green, J. C.; McIndoe, J. S.; Raithby, P. R.; Kociok-Kohn, G.; Weller, A. S. *J. Am. Chem. Soc.* **2006**, *128*, 6247–6263.

- (21) Lin, Z. Y.; Fan, M. F. In *Structural and Electronic Paradigms in Cluster Chemistry*; 1997; Vol. 87.
 (22) Lin, Z.; Williams, I. D. *Polyhedron* **1996**, *15*, 3277–3287.
 (23) Brayshaw, S. K.; Ingleson, M. J.; Green, J. C.; Raithby, P. R.; Kociok-Kohn, G.; McIndoe, J. S.; Weller, A. S. *Angew. Chem., Int. Ed.* **2005**, *44*, 6875–6878.
 (24) Adams, R. D.; Captain, B. *Angew. Chem., Int. Ed.* **2005**, *44*, 2531–2533.

Scheme 2. Hydride Clusters $[\text{Rh}_6(\text{PCy}_3)_6\text{H}_{12}][\text{BAR}^{\text{F}}_4]_2$, **Cy-[H12]²⁺**, and $[\text{Rh}_6(\text{PCy}_3)_6\text{H}_{16}][\text{BAR}^{\text{F}}_4]_2$, **Cy-[H16]²⁺**

to kinetic stabilization afforded toward hydrogen loss by the bulkier cyclohexyl groups, as electronically both clusters would be expected to be very similar. Although cluster complexes with hydride ligands are common, those that can reversibly take up and release H_2 are few.^{25–30} Both DFT calculations and H/D exchange experiments are strongly suggestive of two dihydrogen ligands on the cluster surface of this 16-hydride species;²⁰ and the average interaction energy of the two extra H_2 molecules with the cluster is calculated to be 0.62 eV (60 kJ mol⁻¹) per dihydrogen.³⁴ This is comparable with the binding energy both calculated and experimentally determined for dihydrogen bound to a single metal center (~60–100 kJ mol⁻¹).³¹

The four electrons that can fill the low-lying e_g set in **[H12]²⁺** do not have to come from two bonding pairs in H_2 . In principle they can also arise from simple addition of electrons by electrochemical or chemical reduction (as in the facile uptake of electrons into an unoccupied e_g set in $[\text{Pt}_6(\mu\text{-P}^t\text{Bu}_2)_4(\text{CO})_6][\text{CF}_3\text{SO}_3]_2$).³² In this respect the structural and electronic analogies between $[\text{Rh}_6(\text{PR}_3)_6\text{H}_{12}][\text{BAR}^{\text{F}}_4]_2$ and clusters with π -donating ligands should extend to the observation of sequential redox events. We report here that this is the case. The clusters $[\text{Rh}_6(\text{PR}_3)_6\text{H}_{12}][\text{BAR}^{\text{F}}_4]_2$ show a reversible set of redox processes by cyclic voltammetry, two reductions and an oxidation, and we demonstrate using chemical reductants that the products of sequential addition of electrons can be isolated and fully characterized. We also comment on the ability of these reduced species to take up dihydrogen and conclude by showing that hydrogen uptake and release in these clusters can be switched electrochemically, demonstrating a new concept in the storage and release of dihydrogen that has implications for the emerging hydrogen economy.³³ Aspects of this work have been communicated previously.³⁴

Results and Discussion

Electrochemistry of $[\text{Rh}_6(\text{PCy}_3)_6\text{H}_{12}][\text{BAR}^{\text{F}}_4]_2$. Electrochemical investigations were performed in CH_2Cl_2 solvent using 0.01 M $[\text{NBu}_4][\text{BAR}^{\text{F}}_4]$ ^{35,36} as a supporting electrolyte, as use of the more common $[\text{NBu}_4][\text{PF}_6]$ led to cluster decomposition, presumably by attack of the hexafluorophosphate anion (or fluoride derived from hydrolysis of this anion) on the cluster. Figure 2 shows the cyclic voltammogram of $[\text{Rh}_6(\text{PCy}_3)_6\text{H}_{12}][\text{BAR}^{\text{F}}_4]_2$ **Cy-[H12]²⁺** in CH_2Cl_2 solution. An equivalent voltammogram was obtained for $[\text{Rh}_6(\text{P}^t\text{Pr}_3)_6\text{H}_{12}][\text{BAR}^{\text{F}}_4]_2$ (see Supporting Information), but as this also indicated signs of decomposition we restrict the following discussion to the tricyclohexylphosphine cluster.

Two chemically reversible reduction events are apparent, consistent with **Cy-[H12]^{2+/1+}** and **Cy-[H12]^{1+/0}**, at $E_{1/2} = -0.59$ V ($\Delta E_p = 130$ mV) and $E_{1/2} = -1.51$ V ($\Delta E_p = 140$ mV) versus $(\eta^5\text{-C}_5\text{H}_5)_2\text{Fe}^{0/+}$. The peak to peak separations (ΔE_p) are dominated by ohmic effects, and all these processes are close to reversible. A single, one-electron oxidation at $E_{1/2} = +0.44$ V ($\Delta E_p = 220$ mV) is assigned to **Cy-[H12]^{2+/3+}**, and the larger peak to peak separation for this electron-transfer process indicates quasireversible characteristics. Microelectrode experiments (see Experimental Section) confirmed the consumption of one electron per redox event. Although all the redox states of the cluster are potentially chemically accessible, we demonstrate later that only the reductions led to products that could be isolated.

Consideration of the frontier molecular orbitals of **[H12]²⁺** shows that sequential addition of electrons affords the electronic configurations shown in Scheme 3. For **[H12]** two possible spin states ($S = 1$ or $S = 0$) are conceptually possible, depending on the occupation of the e_g set of orbitals.

Synthesis, Characterization, and Solid-state Structures of the Reduced Clusters. Addition of the oxidant $[\text{N}(\text{C}_6\text{H}_4\text{Br}-4)_3][\text{B}(\text{C}_6\text{F}_5)_4]$ ^{37,38} ($E_{1/2} = +0.70$ V) to $[\text{Rh}_6(\text{PCy}_3)_6\text{H}_{12}][\text{B}(\text{C}_6\text{F}_5)_4]_2$, **Cy-[H12]²⁺**, did not result in the isolation of the electrochemically observed **[H12]³⁺**. Although ¹H and ³¹P NMR spectroscopy indicated the formation of a paramagnetic species, attempts to isolate material only resulted in **Cy-[H12]²⁺** and other decomposition products (by NMR and electrospray ionization mass spectrometry, ESI-MS). Significantly more success was achieved with the chemical reductions. Inspection

(25) Aubart, M. A.; Chandler, B. D.; Gould, R. A. T.; Krogstad, D. A.; Schoondergang, M. F. J.; Pignolet, L. H. *Inorg. Chem.* **1994**, *33*, 3724–3734.

(26) Adams, R. D.; Captain, B.; Smith, M. D. *Angew. Chem., Int. Ed.* **2006**, *45*, 1109–1112.

(27) Safarowic, F. J.; Biedeman, D. J.; Keister, J. B. *J. Am. Chem. Soc.* **1996**, *118*, 11805–11812.

(28) Arif, A. M.; Bright, T. A.; Jones, R. A.; Nunn, C. M. *J. Am. Chem. Soc.* **1988**, *110*, 6894–6895.

(29) Farrugia, L. J.; Green, M.; Hankey, D. R.; Orpen, A. G.; Stone, F. G. A. *J. Chem. Soc., Chem. Commun.* **1983**, 310–312.

(30) Green, M. L. H.; Mountford, P. *J. Chem. Soc., Chem. Commun.* **1989**, 732–734.

(31) Kubas, G. J. *Metal Dihydrogen and σ -Bond Complexes*; Kluwer Academic/Plenum Publishers: New York, 2001.

(32) de Biani, F. F.; Ienco, A.; Laschi, F.; Leoni, P.; Marchetti, F.; Marchetti, L.; Mealli, C.; Zanello, P. *J. Am. Chem. Soc.* **2005**, *127*, 3076–3089.

(33) Schlapbach, L.; Züttel, A. *Nature* **2001**, *414*, 353–358.

(34) Brayshaw, S. K.; Green, J. C.; Hazari, N.; McIndoe, J. S.; Marken, F.; Raithby, P. R.; Weller, A. S. *Angew. Chem., Int. Ed.* **2006**, *45*, 6005–6008.

(35) LeSuer, R. J.; Buttolph, C.; Geiger, W. E. *Anal. Chem.* **2004**, *76*, 6395–6401.

(36) LeSuer, R. J.; Geiger, W. E. *Angew. Chem., Int. Ed.* **2000**, *39*, 248–250.

(37) Connelly, N. G.; Geiger, W. E. *Chem. Rev.* **1996**, *96*, 877–910.

(38) O'Connor, A. R.; Nataro, C.; Golen, J. A.; Rheingold, A. L. *J. Organomet. Chem.* **2004**, *689*, 2411–2414.

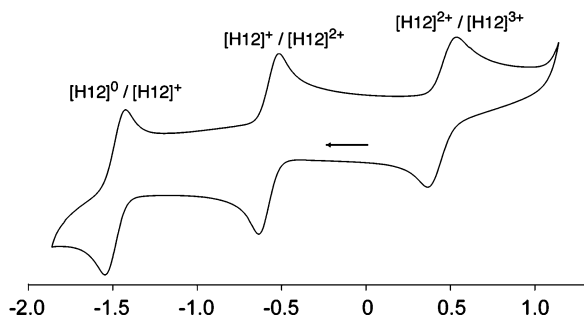
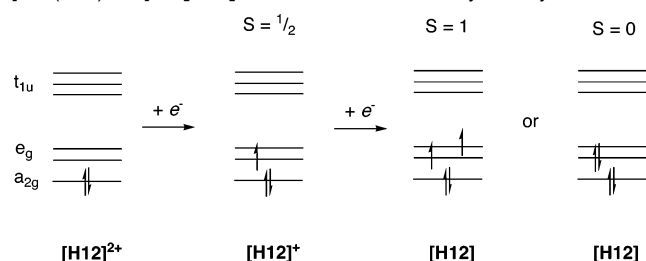


Figure 2. Cyclic voltammogram of 0.32 mM solution of **Cy-[H12]²⁺** showing the three redox processes (CH_2Cl_2 solution, 0.01 M $[\text{NBu}_4][\text{BAR}^{\text{F}_4}]$ electrolyte, 3 mm diameter glassy carbon electrode, sweep rate 100 mV s^{-1}).

Scheme 3. Sequential Addition of Electrons to the Cluster $[\text{Rh}_6(\text{PR}_3)_6\text{H}_{12}]^{2+}$, $[\text{H12}]^{2+}$, under Idealized O_h Symmetry



of the cyclic voltammogram suggested that $\text{Cr}(\eta^6\text{-C}_6\text{H}_6)_2$ ($E_{1/2} = -1.15$ V) would be a suitable chemical reductant to isolate **Cy-[H12]⁺**. Addition of excess (ca. 2 equiv) of $\text{Cr}(\eta^6\text{-C}_6\text{H}_6)_2$ to a difluorobenzene solution of **Cy-[H12]²⁺** and recrystallisation afforded $[\text{Rh}_6(\text{PCy}_3)_6\text{H}_{12}][\text{BAR}^{\text{F}_4}]$, **Cy-[H12]⁺**, in good (76%) isolated yield, which was characterized by NMR, ESR, ESI-MS, microanalysis, and single-crystal X-ray diffraction (Scheme 4).

The ^1H NMR spectrum of **Cy-[H12]⁺** shows no hydride resonances, consistent with a radical species in which the unpaired electron is metal-based. An Evans measurement³⁹ (in CH_2Cl_2) gave an effective magnetic moment of $\mu_{\text{eff}} = 1.82$ BM, close to the value expected for a single unpaired electron ($\mu_{\text{eff}} = 1.73$ BM). The cyclohexyl phosphine protons are paramagnetically shifted and broadened, and a 6:6:6:180 relative ratio is observed. The three resonances which integrate to six protons each are centered at δ 35.7 (fwhm 430 Hz), 16.5 (fwhm 275 Hz), and 5.4 (fwhm 380 Hz), respectively. We explain this pattern by hindered rotation of the triscyclohexylphosphine groups that affords three *ipso*-CH environments orientated differently with regard to the cluster core. Hindered rotation of the bulky phosphine groups is also observed in the diamagnetic

Scheme 4

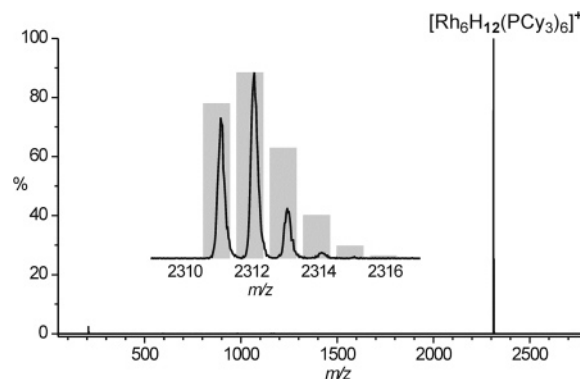
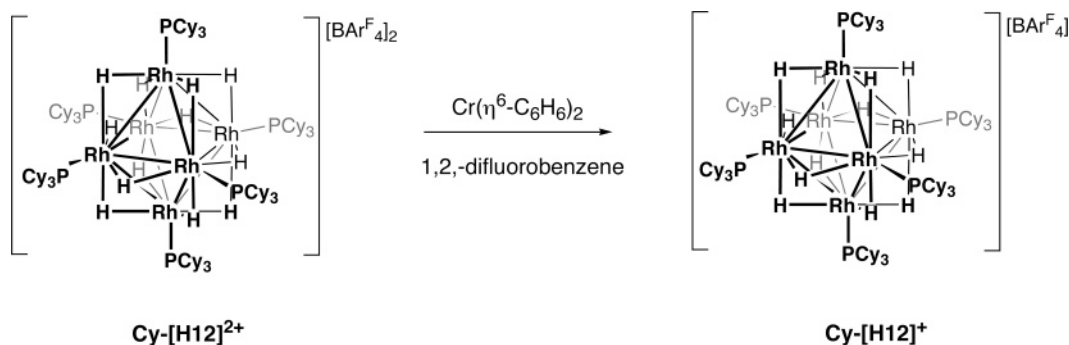


Figure 3. ESI-MS spectrum of **Cy-[H12]⁺**. Inset shows calculated (gray bars) and observed isotope distribution patterns.

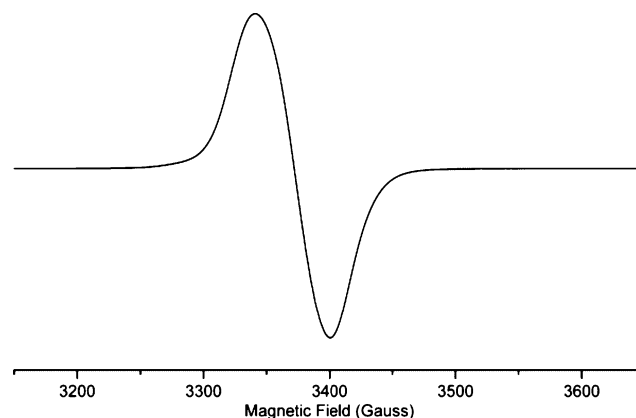


Figure 4. X-band EPR spectrum of **Cy-[H12]⁺** (298 K, 1,2- $\text{C}_6\text{H}_4\text{F}_2$).

precursor **Cy-[H12]²⁺**.²⁰ As expected for a radical species no resonances were observed in the $^{31}\text{P}\{^1\text{H}\}$ NMR spectrum. ESI-MS showed the expected isotope pattern (m/z 2310.9 calcd, 2311.1 obsd) which is consistent with a monocation (Figure 3). The ESR spectrum (Figure 4) showed an isotropic and strong signal with a g value close to free spin (2.010), indicating the unmistakable presence of an unpaired electron in the sample. Addition of the oxidant $[\text{Fe}(\eta^5\text{-C}_5\text{H}_5)_2][\text{BAR}^{\text{F}_4}]$ ⁴⁰ to a CH_2Cl_2 solution of **Cy-[H12]⁺** regenerates the cation **Cy-[H12]²⁺**, showing that this redox couple is chemically reversible.

The solid-state structure of **Cy-[H12]⁺** confirms the monocationic formulation of the cluster, with only one $[\text{BAR}^{\text{F}_4}]^-$ anion associated with each rhodium octahedron (Figure 5). The crystallographic analysis also shows there are two independent cation/anion pairs in the solid state. Bond lengths and angles are effectively the same in both. Both clusters have crystallographically imposed C_2 symmetry in which the 2-fold axis

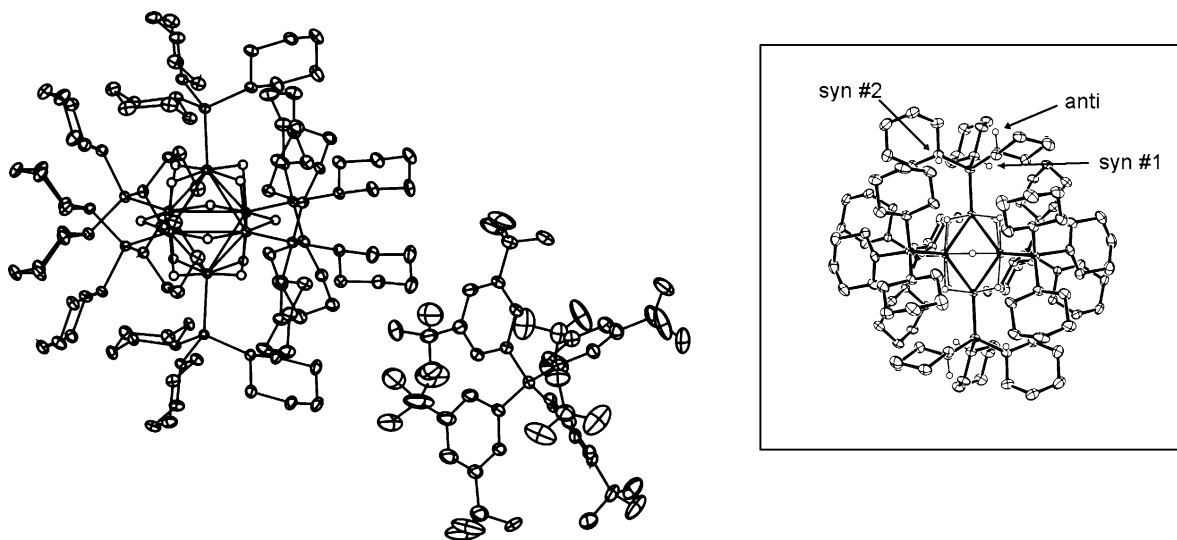


Figure 5. Solid-state structure of **Cy-[H12][BARF₄]** (50% thermal ellipsoids) showing one of the crystallographically independent ion pairs. Inset shows an alternative view of the cationic core down the crystallographic C_2 axis. Arrows indicate the three different *ipso*-CH environments with respect to the cluster core: two *syn* and one *anti*.

Table 1. Comparison of Cluster-Core Metrics for Complexes **Cy-[H12]²⁺**, **Cy-[H12]⁺**, and **ⁱPr-[H12]**

	Cy-[H12]²⁺ ^b	Cy-[Rh₆(PCy₃)₆H₁₂]⁺, [H12]⁺ ^c	ⁱPr-[H12]
Rh–Rh mean, Å	2.735(1)	2.735(1), 2.735(1)	2.741(1)
Rh–Rh, Å	2.743(1)–2.719(1)	2.753(1)–2.707(1) 2.750(1)–2.720(1)	2.742(1)–2.739(1)
δ (Rh–Rh), Å ^a	0.024	0.046, 0.030	0.003
Rh···Rh cross-cluster, Å	3.869(1)–3.858(1)	3.870–3.866 3.909–3.851	3.875
δ (Rh···Rh), Å	0.011	0.004, 0.058	n/a
P···P cross-cluster	8.392–8.379	8.367–8.365 8.425–8.347	8.328
δ (P···P), deg ^a	0.013	0.002, 0.078	0
Rh–P mean, Å	2.262(1)	2.254(1), 2.251(1)	2.227(1)
Rh···Rh–P, deg	178.3(1)–177.3(1)	177.9(1)–176.9(1) 177.6(1)–176.6(1)	177.5(1)
Rh–H, Å	1.89(5)–1.66(5)	1.87(4)–1.68(4) 1.86(3)–1.71(3)	1.70(2)–1.78(2)

^a Maximum deviation in distances. ^b Data taken from ref 20. This paper also presents metric data for **ⁱPr-[H12]²⁺**. ^c Two crystallographically independent molecules in the unit cell.

bisects two opposite Rh–Rh bonds. Table 1 presents selected metric data for **Cy-[H12]⁺**, alongside that for the precursor cluster **Cy-[H12]²⁺**. These show that there is no major change in the cluster core on addition of a single electron, the only notable difference being that that Rh–P distances contract slightly (ca. 0.01 Å). The lack of significant structural change is consistent with the addition of an electron to a nonbonding Rh–Rh orbital (Figure 1).²⁰ The hydride ligands in **Cy-[H12]⁺** were all located in the final difference electron density map, and within error they bridge each Rh–Rh edge symmetrically. With regard to the ¹H NMR spectrum that suggests three different *ipso*-CH cyclohexyl environments, close inspection of the structure of **Cy-[H12]⁺** reveals that for each phosphine the cyclohexyl rings adopt three different orientations leading to three *ipso*-CH environments, two pointing more toward the cluster core (*syn*) and one pointing away (*anti*). This pattern is repeated for each phosphine ligand and, if retained in solution (i.e., the phosphine ligands were locked toward rotation), would lead to a 6:6:6 pattern in the ¹H NMR spectrum for these hydrogen atoms, as is observed.

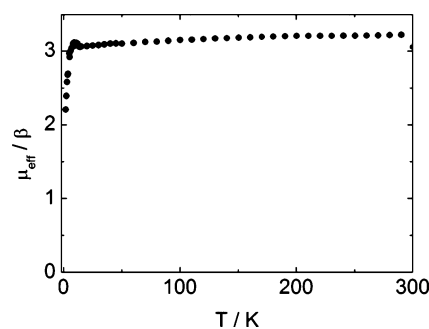


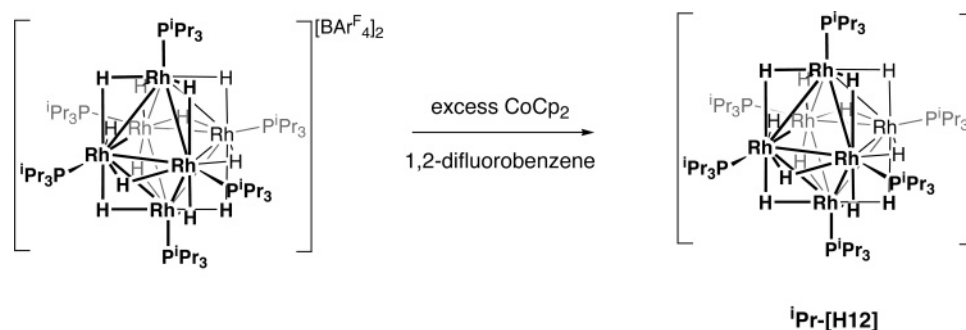
Figure 6. Variable-temperature magnetic data for compound **ⁱPr-[H12]**.

Addition of excess $\text{Co}(\eta^5\text{-C}_5\text{H}_5)_2$ ($E_{1/2} = -1.33$ V) or $\text{Co}(\eta^5\text{-C}_5\text{Me}_5)_2$ ($E_{1/2} = -1.94$ V) to **Cy-[H12]²⁺** resulted in a paramagnetic species that showed a ¹H NMR spectrum similar to that of **Cy-[H12]⁺**. Attempts to isolate a pure, neutral, product failed due to the low solubility in pentane or toluene meaning that removal of ionic byproducts was not possible. However, addition of excess $\text{Co}(\eta^5\text{-C}_5\text{H}_5)_2$ to $[\text{Rh}_6(\text{P}^i\text{Pr}_3)_6\text{H}_{12}][\text{BARF}_4]_2$ in 1,2-difluorobenzene ultimately resulted in a pentane-soluble blue-green product that could be recrystallized in moderate yield (56%) from cold pentane and was identified as the neutral cluster

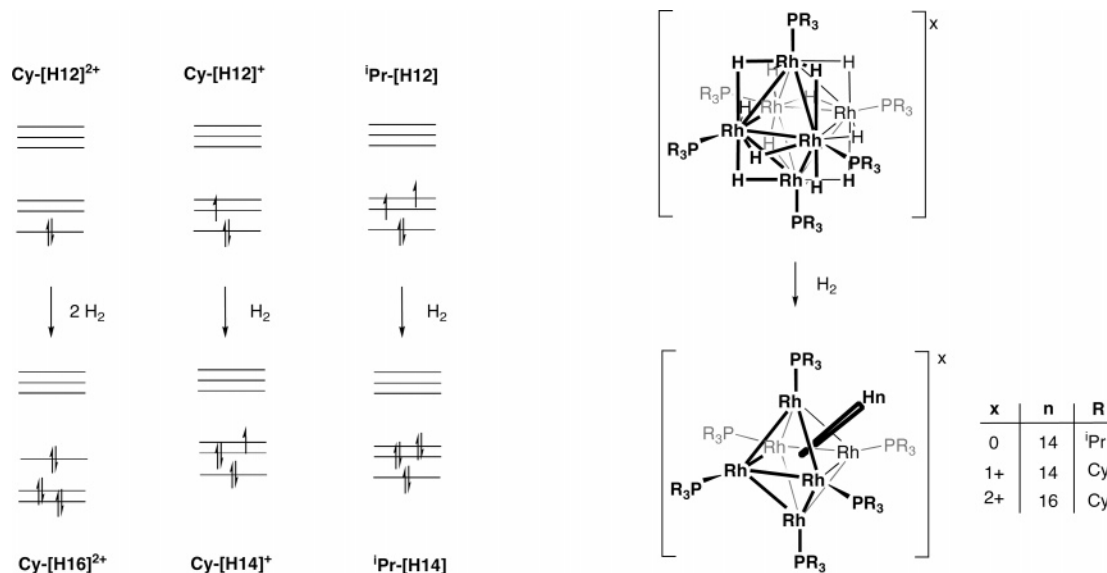
(39) Evans, D. F. *J. Chem. Soc.* **1959**, 2003–2005.

(40) Calderazzo, F.; Pampaloni, G.; Rocchi, L.; Englert, U. *Organometallics* **1994**, *13*, 2592–2601.

Scheme 5



Scheme 6. Frontier Molecular Orbital Occupancies on Sequential Addition of Dihydrogen (i.e., One Bonding Electron Pair) to the Clusters $\text{Cy-[H12]}^{1+/2+}$ and iPr-[H12] under Idealized O_h Symmetry



$\text{Rh}_6(\text{P}^i\text{Pr}_3)_{12}\text{H}_{12}$, iPr-[H12] (Scheme 5). Although cobaltocene should not be able to effect a two-electron reduction ($E_{1/2} -1.33$ V versus -1.51 V for $[\text{H12}]^{0/+}$), we suggest that preferential crystallization of iPr-[H12] from cold difluorobenzene solution during workup, which also contains excess $\text{Co}(\eta^5\text{-C}_5\text{H}_5)_2$ and iPr-[H12]^+ , drives the reduction to completion. Use of the stronger reducing agent $\text{Co}(\eta^5\text{-C}_5\text{Me}_5)_2$ resulted in difficulties in purification due to the similarities in solubility between reductant and product.

Addition of two electrons to iPr-[H12] can conceptually result in two possible electronic configurations. If the two electrons occupy a single e_g orbital then an $S = 0$ ground state results, and the cluster is diamagnetic. Alternatively, one electron in each e_g orbital would result in an $S = 1$ ground state and a paramagnetic cluster. ^1H NMR spectroscopy is consistent with a paramagnetic complex and thus a $S = 1$ groundstate. The hydride ligands are not observed, while the methine isopropyl protons are observed as a single, broad, paramagnetically shifted resonance at δ 30.87 (18 H, fwhm 83 Hz). Unlike Cy-[H12]^+ restricted rotation of the slightly smaller *tris*-isopropylphosphine groups is not observed, just as in the diamagnetic precursor $[\text{Rh}_6(\text{P}^i\text{Pr}_3)_{12}\text{H}_{12}][\text{BARF}_4]_2$.²⁰ Evans measurements (toluene) afforded an effective magnetic moment of $\mu_{\text{eff}} = 2.89$ BM, close to the value predicted for 2 unpaired electrons ($\mu_{\text{eff}} = 2.83$ BM). Surprisingly, EPR measurements, even at very low temperatures (5–10 K), gave featureless spectra. The $S = 1$ ground state was unequivocally confirmed by variable temperature magnetic

susceptibility measurements. Figure 6 shows the temperature dependence of μ_{eff} for iPr-[H12] measured in an applied magnetic field of 1 T. The moment observed at room temperature is reasonable for an $S = 1$ system with two unpaired electrons, and there is essentially no variation in μ_{eff} at temperatures down to 5 K. Interestingly below 5 K, μ_{eff} starts to drop off which might be indicative of a singlet ground state at very low temperatures or weak, antiferromagnetic coupling between the clusters. Alternatively a gross structural rearrangement of the hydride ligands, forming a molecule with lower symmetry at very low temperature, could also account for the observed magnetic behavior. The $S = 1$ groundstate observed in iPr-[H12] is in contrast to diamagnetic ($S = 0$) $\text{Pt}_6(\mu\text{-P}^i\text{Bu}_2)_4\text{(CO)}_6$ which is formed on a two-electron reduction of a dicationic precursor which has a degenerate e_g set of LUMOs. In this case a Jahn–Teller distortion is suggested to be operating.³²

The solid-state structure of iPr-[H12] is shown in Figure 7 and confirms the neutral cluster core. In the solid-state, iPr-[H12] crystallizes in the rhombohedral space group $R\bar{3}$, and this leads to each cluster $\{\text{Rh}(\text{P}^i\text{Pr}_3)\}$ vertex being crystallographically identical. The high symmetry associated with the molecule also means that there are only two crystallographically distinct hydride environments. These two different hydrides both span the Rh–Rh edges symmetrically as determined within the limits of the X-ray diffraction experiment. On reduction, compared to iPr-[H12]^{2+} ²⁰ the mean Rh–Rh distances become marginally longer [2.741 and 2.720 Å in iPr-[H12] and iPr-[H12]^{2+} ,

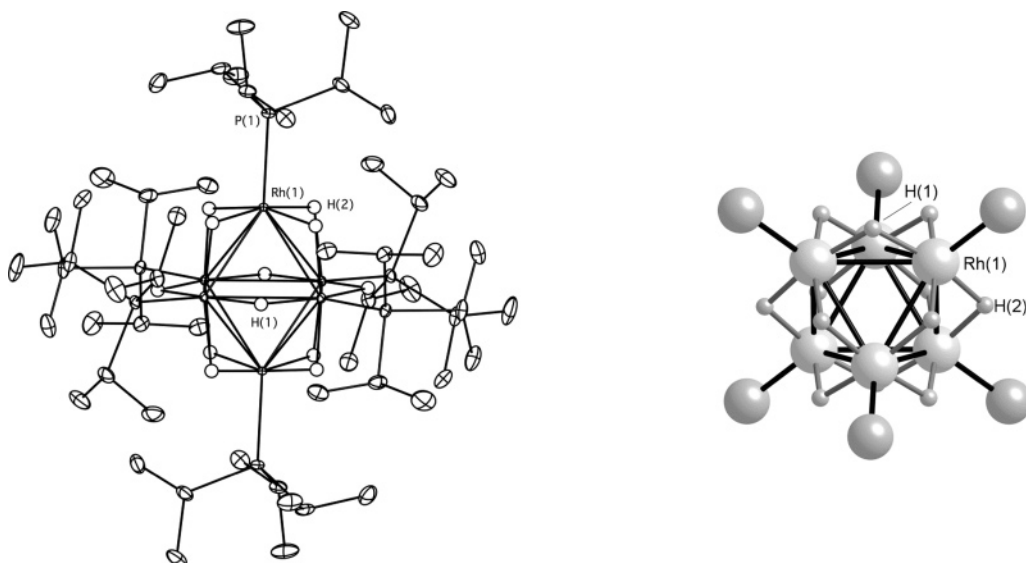


Figure 7. Solid-state structure of neutral $i\text{Pr}[\text{H}12]$ (50% thermal ellipsoids), showing atom labeling scheme. Inset shows an expanded view of the metal core viewed down the C_{3v} axis that demonstrates the two different hydride environments H(1) and H(2) imposed by crystallographic symmetry.

respectively] and the mean Rh–P distances become slightly smaller [2.227 and 2.246 Å, respectively]. This latter observation continues the trend observed in $\text{Cy}[\text{H}12]^+$.

Dihydrogen Uptake by the Clusters $[\text{Rh}_6(\text{PR}_3)_6\text{H}_{12}]^{0/+}$. The reversible uptake of hydrogen by molecular or extended materials (such as nanoclusters) is an area that is attracting significant current interest, and much of this interest has centered on the role that such species play in hydrogenation reactions (especially arene hydrogenation), in particular the nature of the actual species in catalysis (nanocluster versus molecular cluster),^{41–46} and potential hydrogen storage applications.^{33,47–51} We have recently demonstrated that the clusters $[\text{Rh}_6(\text{PR}_3)_6\text{H}_{12}]$ – $[\text{BAR}^{\text{F}}_4]_2$ reversibly take up two molecules of H_2 under ambient (1 atm H_2) conditions as a result of their electronic structure which contains two low lying, empty orbitals. Although reduction of these clusters adds electrons to these orbitals, they do not become fully filled and thus we reasoned that the reduced clusters should still be able to take up H_2 (Scheme 6).

Addition of H_2 (1 atm) to a CH_2Cl_2 solution of $\text{Cy}[\text{H}12]^+$ led to uptake of H_2 . Although the ^1H NMR spectrum of the product demonstrated a paramagnetic species, and the $^{31}\text{P}\{^1\text{H}\}$ NMR spectrum was featureless, ESI-MS showed the formation of the 14-hydride species $[\text{Rh}_6(\text{PCy}_3)_6\text{H}_{14}]^+$ (m/z calcd 2312.9, obsd 2313.1) and UV–visible spectroscopy (Supporting Information) showed a distinct change in the electronic absorption spectrum on addition of H_2 . Efforts to isolate $\text{Cy}[\text{H}14]^+$ always

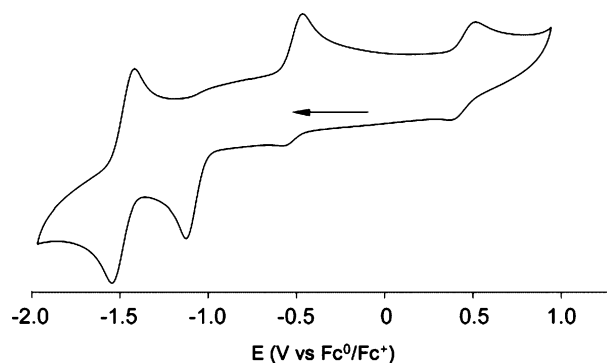


Figure 8. Cyclic voltammogram of 0.32 mM $\text{Cy}[\text{H}16]^{2+}$ (CH_2Cl_2 solution, 0.01 M $[\text{NBu}_4][\text{BAR}^{\text{F}}_4]$ electrolyte, 3 mm diameter glassy carbon electrode, sweep rate 100 mV s^{-1}). Arrow indicates the approximate start of the experiment.

led to loss of H_2 and the formation of $\text{Cy}[\text{H}12]^+$. Calculations³⁴ suggest that the structure of $[\text{H}14]^+$ has a dihydrogen ligand on the surface, similar to the structure suggested for $[\text{H}16]^{2+}$.²⁰ Addition of D_2 to a CH_2Cl_2 solution of $\text{Cy}[\text{H}14]^+$ results in the slow (hours) appearance of H_2 and HD in the ^1H NMR spectrum, which is consistent with, although not unambiguous proof of, energetically accessible dihydrogen on the cluster surface.³¹

In contrast to the paramagnetism of $\text{Cy}[\text{H}14]^+$, addition of H_2 to neutral $i\text{Pr}[\text{H}12]$ results in a diamagnetic cluster species which we assign as $i\text{Pr}[\text{H}14]$. This diamagnetism is fully consistent with the addition of an electron pair to the e_g orbitals in $i\text{Pr}[\text{H}12]$, which has a triplet spin state. Presumably H_2 addition occurs via a higher energy singlet intermediate, although we have not investigated this computationally. Examples exist of H_2 addition to triplet ground state complexes to form a singlet, diamagnetic, hydride product; for example addition of H_2 to $\text{WH}\{\text{N}(\text{CH}_2\text{CH}_2\text{SiMe}_3)_3\}$.⁵² This reaction has been put forward as an example of “spin-blocking”, where there is a significant barrier along the reaction coordinate

- (41) Hagen, C. M.; Widegren, J. A.; Maitlis, P. M.; Finke, R. G. *J. Am. Chem. Soc.* **2005**, *127*, 4423–4432.
 (42) Hagen, C. M.; Vieille-Petit, L.; Laurency, G.; Suss-Fink, G.; Finke, R. G. *Organometallics* **2005**, *24*, 1819–1831.
 (43) Dumestre, F.; Chaudret, B.; Amiens, C.; Renaud, P.; Fejes, P. *Science* **2004**, *303*, 821–823.
 (44) Thomas, J. M.; Johnson, B. F. G.; Raja, R.; Sankar, G.; Midgley, P. A. *Acc. Chem. Res.* **2003**, *36*, 20–30.
 (45) Dyson, P. J. *Dalton Trans.* **2003**, 2964–2974.
 (46) *Metal Clusters in Chemistry*; Braunstein, P., Oro, L. A., Raithby, P. R., Eds.; Wiley-VCH: Weinheim, 1999.
 (47) Dincă, M.; Long, J. R. *J. Am. Chem. Soc.* **2005**, *127*, 9376–9377.
 (48) Kaye, S. S.; Long, J. R. *J. Am. Chem. Soc.* **2005**, *127*, 6506–6507.
 (49) Rowsell, J. L. C.; Eckert, J.; Yaghi, O. M. *J. Am. Chem. Soc.* **2005**, *127*, 14904–14910.
 (50) Zhao, X.; Xiao, B.; Fletcher, A. J.; Thomas, K. M.; Bradshaw, D.; Rosseinsky, M. J. *Science* **2004**, *306*, 1012–1015.
 (51) Wong-Foy, A. G.; Matzger, A. J.; Yaghi, O. M. *J. Am. Chem. Soc.* **2006**, *128*, 3494–3495.

- (52) Schrock, R. R.; Shih, K. Y.; Dobbs, D. A.; Davis, W. M. *J. Am. Chem. Soc.* **1995**, *117*, 6609–6610.

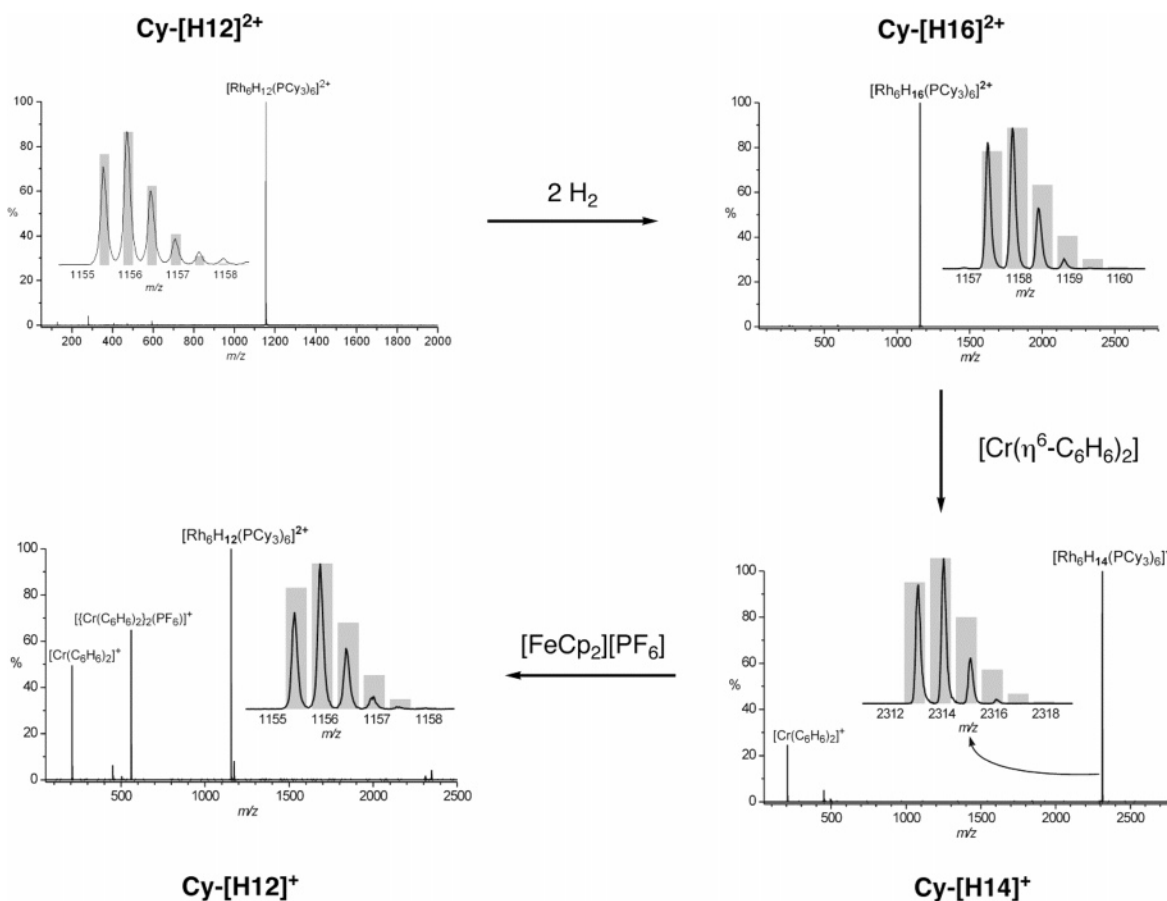


Figure 9. ESI-MS data for the bulk chemical redox hydrogen store cycle in CH_2Cl_2 . Apart from clusters, the only other species observed arise from the reducing and oxidizing agents. For full details, see Experimental Section.

induced by a spin change.⁵³ Although we are not in a position to comment in detail on the possibility of such a process occurring here, it is interesting to note that H_2 addition is significantly slower for $i\text{Pr}-[\text{H12}]$ (16 h at 4 atm H_2) than that for $\text{Cy}-[\text{H12}]^{2+}$ (effectively instantaneous under the same conditions).²⁰ Also the back, dehydrogenation, reaction with 1-hexene is not observed to proceed, whereas for $\text{Cy}-[\text{H16}]^{2+}$ this is facile, in agreement with spin change arguments. Consistent with a diamagnetic formulation, the ^1H NMR spectrum of $i\text{Pr}-[\text{H14}]$ shows no paramagnetically shifted resonances. In the high-field region a broad hydride resonance at $\delta -25.6$ is observed that integrates consistently to only 13 H (12.9 H) relative to the isopropyl groups, rather than the expected 14 H. This slightly low integral (by 7%) could be a reflection of the broadness of the peak and the inherent difficulties in accurately determining hydride integral values, but it could also suggest a structure with 13 mutually exchanging surface hydride ligands and one (broad and unobserved) interstitial hydride.^{54–56} Indeed we have commented on a similar arrangement of the hydride ligands for $[\text{Rh}_6(\text{PR}_3)_6\text{H}_{16}][\text{BAR}^{\text{F}}_4]$.²⁰

The room temperature $^{31}\text{P}\{^1\text{H}\}$ NMR spectrum shows a single broad peak. At low temperature the $^{31}\text{P}\{^1\text{H}\}$ NMR (250 K) spectrum reveals two sharper signals in the ratio 2:5 that both display Rh–P coupling. At this temperature the ^1H NMR spectrum displays two hydride environments also in the approximate 2:5 ratio. Further cooling (200 K) results a 1:1.5 ratio in both the $^{31}\text{P}\{^1\text{H}\}$ and ^1H NMR spectra in the hydride region. The overall hydride integral value remains approximately 13 H. This temperature-dependent behavior suggests two isomers in solution, both having exchanging hydride ligands. Longitudinal relaxation time measurements (T_1) revealed a minimum value for these hydride signals of 72 ms at 250 K (400 MHz). This relatively short relaxation time could suggest exchange between hydride and dihydrogen ligands at this temperature. Similar exchange is observed for $[\text{Ir}(\text{H})_2(\eta^2\text{-H}_2)_2(\text{PCy}_3)_2]^+$ and $\text{Ru}(\text{H})_2(\eta^2\text{-H}_2)_2(\text{PCy}_3)_2$.^{57–59} Intact cluster dihydrogen ligands have been suggested in $[\text{H}_6\text{Ru}_4(\text{C}_6\text{H}_6)_4]^{2+}$ on the basis of a T_1 measurement of 34 ms at 200 MHz.⁶⁰ Given that T_1 depends linearly on field strength,⁶¹ this value is similar to the one we observe at 400 MHz. Addition of D_2 (1 atm, 313 K) to $i\text{Pr}-[\text{H12}]$ slowly (4 days) results in the formation of $\text{HD}_{(g)}$ and the

(53) Carreon-Macedo, J. L.; Harvey, J. N. *J. Am. Chem. Soc.* **2004**, *126*, 5789–5797.

(54) Hart, D. W.; Teller, R. G.; Wei, C. Y.; Bau, R.; Longoni, G.; Campanella, S.; Chini, P.; Koetzle, T. F. *J. Am. Chem. Soc.* **1981**, *103*, 1458–1466.

(55) Jackson, P. F.; Johnson, B. F. G.; Lewis, J.; Raithby, P. R.; McPartlin, M.; Nelson, W. J. H.; Rouse, K. D.; Allibon, J.; Mason, S. A. *J. Chem. Soc., Chem. Commun.* **1980**, 295–297.

(56) Eguchi, T.; Heaton, B. T.; Harding, R.; Miyagi, K.; Longoni, G.; Nahrung, J.; Nakamura, N.; Nakayama, H.; Pakkanen, T. A.; Pursiainen, J.; Smith, A. K. *J. Chem. Soc., Dalton Trans.* **1996**, 625–630.

(57) Sabo-Etienne, S.; Chaudret, B. *Coord. Chem. Rev.* **1998**, *180*, 381–407.

(58) Crabtree, R. H.; Lavin, M.; Bonneviot, L. *J. Am. Chem. Soc.* **1986**, *108*, 4032–4037.

(59) Chaudret, B.; Devillers, J.; Poilblanc, R. *Organometallics* **1985**, *4*, 1727–1732.

(60) Suss-Fink, G.; Plasseraud, L.; Maise-Francois, A.; Stoeckli-Evans, H.; Berke, H.; Fox, T.; Gautier, R.; Saillard, J. Y. *J. Organomet. Chem.* **2000**, *609*, 196–203.

(61) Crabtree, R. H. *Acc. Chem. Res.* **1990**, *23*, 95–101.

Table 2. Crystal and Structure Refinement Data for the New Cluster Compounds

compound	Cy-[H12][BARf ₄]-5.5(C ₆ H ₅ CH ₃)	¹ Pr-[H12]
empirical formula	C _{178.50} H _{265.50} BF ₂₄ P ₆ Rh ₆	C ₅₄ H ₁₃₆ P ₆ Rh ₆
formula weight	3681.50	1590.92
temperature	150(2)	150(2)
wavelength/Å	0.710 73	0.8460
crystal system	monoclinic	rhombohedral
space group	P2/n	R3
a / Å	20.3420(1)	13.4673(5)
b / Å	24.4480(2)	13.4673(5)
c / Å	35.3600(3)	33.922(2)
α / deg	90	90
β / deg	90.13	90
γ / deg	90	90
volume / Å ³	17585.2(2)	5328.1(5)
Z	4	3
density (calculated) / mg/m ³	1.391	1.489
absorption coefficient / mm ⁻¹	0.679	1.526
F(000)	7670	2466
crystal size / mm ³	0.35 × 0.35 × 0.10	0.10 × 0.10 × 0.05
theta range for data collection / deg	3.53 to 28.70	3.60 to 29.80
reflections collected	188 785	11 064
independent reflections	43989 [R(int) = 0.0595]	2004 [R(int) = 0.0328]
data/restraints/parameters	43 989/23/2222	2004/0/114
largest diff. peak and hole/ e ⁻ Å ⁻³	0.941 and -0.868	0.423 and -0.431
final R ^{a,b} indices [I > 2σ(I)]	R ₁ = 0.0408 wR ₂ = 0.0874	R ₁ = 0.0179 wR ₂ = 0.0454
R ^{a,b} indices (all data)	R ₁ = 0.1000 wR ₂ = 0.1065	R ₁ = 0.0185 wR ₂ = 0.0459
goodness-of-fit on F ^{2c}	1.019	1.052

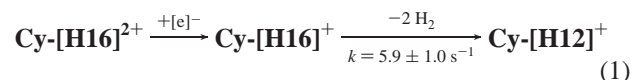
$$^a R_1 = \sum ||F_o| - |F_c|| / \sum |F_o|. \quad ^b wR_2 = \{\sum [w(F_o^2 - F_c^2)^2] / \sum [w(F_o^2)]\}^{1/2}. \quad ^c \text{GOF} = S = \{\sum [w(F_o^2 - F_c^2)^2] / (n - p)\}^{1/2}.$$

complete deuteration of the hydrides on the cluster, and although this is consistent with accessible dihydrogen on the cluster surface it is not unambiguous proof. Whatever the actual arrangement of hydride ligands in ¹Pr-[H14], importantly simple addition of H₂ to paramagnetic ¹Pr-[H12] affords a diamagnetic product fully consistent with the addition of one molecule of H₂ (i.e., one electron pair) to the cluster. UV-vis spectroscopy (see Supporting Informations) showed a subtle, but distinct, change in the electronic absorption spectrum on addition of H₂.

Redox-Promoted Hydrogen Loss. Inspection of the M.O. diagram for [H16]²⁺ (Scheme 6) suggests that addition of one extra electron would result in the population of a high-lying orbital, and this could destabilize the cluster resulting in H₂ loss to re-establish a large HOMO-LUMO gap. If coupled with a sequential oxidation of the cluster, this potentially could lead to the reversible binding and release of H₂, triggered by a single electron redox event. Such a process has implications for the storage of hydrogen for future energy applications.

Figure 8 displays the cyclic voltammogram for Cy-[H16]²⁺ which shows an irreversible one-electron reduction at E_{1/2} -1.00 V, relative to Fe(η⁵-C₅H₅)₂^{0/+}. Progressively increasing the scan rate to 10 V s⁻¹ leads to the observation of the back-oxidation, which yields a half-life for the reduced intermediate of 170 ms at 293 K (or a chemical rate constant k = 5.9 ± 1.0 s⁻¹). The irreversible reduction is followed by a reversible reduction at exactly the same potential as Cy-[H12]^{0/+} (E_{1/2} -1.51 V). The return oxidation sweep also shows Cy-[H12]⁺²⁺ (E_{1/2} -0.59 V) and Cy-[H12]^{2+/3+} (E_{1/2} +0.44 V) with no other new redox event observed. These redox events also show diffusion controlled kinetics. Overall these observations are very strongly suggestive of an electrochemical process in which addition of a single electron to Cy-[H16]²⁺ results in elimination of 2 equiv of H₂ from an unstable intermediate Cy-[H16]⁺ and the formation of Cy-[H12]⁺ (eq 1). Using the fully deuterated

cluster Cy-[D16]²⁺ (prepared from addition of D₂ to Cy-[H16]²⁺ for 3 days)²⁰ resulted in an unchanged cyclic voltammogram. Calculations for the half-life of the reduced intermediate, Cy-[D16]⁺, also afford the same rate constant within error for loss of D₂ from the cluster compared with Cy-[H16]⁺. However, the error in these rates is significant, and thus we are reluctant to state with any confidence whether an isotope effect is, or is not, operating. Kinetic isotope effects have been observed for dihydrogen loss from mononuclear complexes.³¹



Use of a platinum electrode rather than a glassy carbon electrode resulted in a significant reduction in the relative observed current for the irreversible event at E_{1/2} -1.00 V attributed to reduction of Cy-[H12]²⁺ and subsequent H₂ loss from Cy-[H16]⁺, while the redox events associated with Cy-[H12]²⁺ remained unchanged (see Supporting Information). This is presumably due to the facile loss of H₂ to platinum and is not unexpected given the high affinity platinum has for H₂.^{62,63} This observation further underscores that the irreversible redox event is due to H₂ loss. Under a H₂ atmosphere the same redox processes are still observed, notably the irreversible loss of H₂ (see Supporting Information).

These processes may also be followed by ESI-MS, NMR spectroscopy, and chemical redox agents (Figure 9 for ESI-MS spectra). Addition of the reducing agent Cr(η⁶-C₆H₆)₂ (E_{1/2} -1.15 V) to a CH₂Cl₂ solution of Cy-[H16]²⁺ results in the

(62) Gates, B. C. *Chem. Rev.* **1995**, *95*, 511–522.(63) Oudenhuijzen, M. K.; van Bokhoven, J. A.; Miller, J. T.; Ramaker, D. E.; Koningsberger, D. C. *J. Am. Chem. Soc.* **2005**, *127*, 1530–1540.

clean formation of $[\text{Rh}_6(\text{P}(\text{C}_6\text{H}_5)_3)_6\text{H}_{14}][\text{BAr}^{\text{F}_4}] \text{Cy}[\text{H14}]^+$. The starting material $\text{Cy}[\text{H12}]^{2+}$ is simply returned by oxidation of $\text{Cy}[\text{H14}]^+$ using $[\text{Fe}(\eta^5\text{-C}_5\text{H}_5)_2][\text{PF}_6]$ ($E_{1/2}$ 0.00 V) which also results in the elimination of a further equivalent of H_2 . This completes a storage cycle for two molecules of H_2 that is triggered by the simple addition and removal of one electron.

Calculations for this redox cycle show that addition of H_2 to $\text{Cy}[\text{H12}]^{2+}$ to give $\text{Cy}[\text{H16}]^{2+}$ is an overall exothermic process taking two electrons into the degenerate e_g set of LUMO orbitals which also establishes a larger HOMO–LUMO gap.³⁴ Reduction of $\text{Cy}[\text{H16}]^{2+}$ to afford unstable $\text{Cy}[\text{H16}]^+$ results in H_2 loss to re-establish a large SOMO/HOMO–1 gap. Why that on chemical reduction $\text{Cy}[\text{H14}]^+$ is observed, while electrochemically $\text{Cy}[\text{H12}]^+$ is formed, is not clear at the present time. Although there is this subtle change in the order of events between the solution bulk chemical processes and electrochemical processes, the overall redox hydrogen storage/release cycle holds for both: reduction of $\text{Cy}[\text{H16}]^{2+}$ and subsequent reoxidation to afford starting cluster $\text{Cy}[\text{H12}]^{2+}$ is effectively quantitative, cyclable, and involves 2 equiv of H_2 per cluster per cycle. Redox-induced loss of hydrogen or protons has been reported previously. For example irreversible oxidation of the dihydrogen complex $[\text{Co}(\text{P}(\text{CH}_2\text{CH}_2\text{PPh}_2)_3)(\eta^2\text{-H}_2)][\text{PF}_6]$ results in the loss of a proton,⁶⁴ while reduction of the vinylidene complex $[\text{Rh}(\text{C}=\text{CHPh})(\text{N}(\text{CH}_2\text{CH}_2\text{PPh}_2)_3)[\text{BF}_4]$ results in H_2 loss, to form an acetylide.⁶⁵ Redox promoted oxidation of H_2 to afford protons (or the reverse reaction, electrocatalytic generation of H_2) is, of course, also very well documented in the study of hydrogenase chemistry.^{66,67}

Conclusions

We have demonstrated here that structural similarities between $[\text{Rh}_6(\text{PR}_3)_6\text{H}_{12}]^{2+}$ and early transition metal clusters with π -donor ligands extend to the redox chemistry of these clusters, inasmuch that three different redox states of the clusters, $[\text{Rh}_6(\text{PR}_3)_6\text{H}_{12}]^{2+/1+/0}$, can be observed electrochemically and two of these isolated using chemical reductants. These new cluster species arise from simple sequential addition of electrons to the low-lying e_g set of orbitals present in the parent cluster. Furthermore the chemically reduced clusters also take up dihydrogen in an attempt to fill these orbitals. Just as we have suggested for $[\text{Rh}_6(\text{PR}_3)_6\text{H}_{12}]^{2+}$, these reduced clusters can probably be isolated due to the stabilization afforded to the cluster core by the bulky, shrouding, alkyl phosphine groups.²⁰ Pleasingly, the products of uptake of electrons and H_2 can be predicted from both simple consideration of the frontier molecular orbital structure as well as more sophisticated analysis of energies using DFT techniques.^{20,34} Once these orbitals are full in $\text{Cy}[\text{H16}]^{2+}$, addition of a further electron to a high-lying orbital results in the loss of H_2 to re-establish a significant HOMO–LUMO gap. This redox-promoted loss of H_2 in a molecular material, we believe, presents a new method of storing and rapidly releasing H_2 under the attractive conditions of room temperature and pressure.

Hydrogen storage is an area of intense current interest, being driven by the requirements for reversible storage of dihydrogen for future energy applications.³³ Chemisorption of dihydrogen in the form of light metal hydrides is one approach to the problem of storing large amounts of H_2 reversibly.⁶⁸ Physisorption of dihydrogen onto porous network materials such as activated carbon, Metal Organic Framework (MOF) materials,^{47,48,69–71} or related systems^{48,72,73} presents an alternative method. Although significant and elegant advances have been made in both areas, challenges still remain. Metal hydrides require temperature cycling to encourage loss of hydrogen, this being a consequence of the chemisorption of hydrogen (binding energies of >100 kJ mol^{-1}), and while porous networks show reversible H_2 uptake without temperature cycling, they generally require low temperatures (77 K) and an overpressure to retain H_2 , a consequence of the dihydrogen being physisorbed.^{69,71,74} MOF systems that hold onto H_2 at reduced pressure (~ 0.01 atm) have been described, but these also only operate at 77 K.⁵⁰

Given this, a material that both was a true store of hydrogen under ambient conditions of temperature and pressure and released the stored H_2 without significant external thermal energy input would be of fundamental interest. The electrochemical cycle revealed here using clusters based upon $[\text{Rh}_6(\text{PCy}_3)_6\text{H}_{12}]^{2+}$ clearly goes some way to addressing these needs. However, the hydrogen storage capacity by $\text{Cy}[\text{H12}]^{2+}$ is extremely modest, 0.1% w/w, as the cluster and associated anions are of high molecular mass, and this value is clearly not sufficient for practical storage of H_2 [US DOE 2010 target of 6.5% by weight].⁷⁵ This said, the ability to store H_2 at no partial pressure of H_2 (and even under a dynamic vacuum) at 298 K, coupled with the very rapid redox-promoted release of 2 equiv of H_2 that returns the store quantitatively to its “uncharged” state, is, we believe, unique. These attractive features arise due to the special characteristics brought upon the system by the electronic and steric properties of the metal cluster: (i) two low lying unoccupied molecular orbitals available for the uptake of bonding electron pairs from H_2 , (ii) the calculated binding energy of H_2 to the cluster of 60 kJ mol^{-1} (lying at a value intermediate between physisorption and chemisorption regimes), and (iii) the kinetic stabilization afforded toward facile hydrogen loss by the shrouding trialkylphosphine groups.

Experimental Section

General. All manipulations were performed under an inert atmosphere of argon, using standard Schlenk-line and glovebox techniques. Glassware was dried in an oven at 130 °C overnight and flamed with a blowtorch, under a vacuum, three times before use. $\text{C}_6\text{H}_5\text{F}$ and $\text{C}_6\text{H}_4\text{F}_2$ were distilled from CaH_2 . Toluene, CH_2Cl_2 , pentane, and hexane were

- (64) Bianchini, C.; Laschi, F.; Peruzzini, M.; Ottaviani, F. M.; Vacca, A.; Zanello, P. *Inorg. Chem.* **1990**, *29*, 3394–3402.
 (65) Bianchini, C.; Meli, A.; Peruzzini, M.; Zanobini, F.; Zanello, P. *Organometallics* **1990**, *9*, 241.
 (66) Tard, C.; Liu, X. M.; Ibrahim, S. K.; Bruschi, M.; De, Gioia, L.; Davies, S. C.; Yang, X.; Wang, L. S.; Sawers, G.; Pickett, C. J. *Nature* **2005**, *433*, 610–613.
 (67) Mejia-Rodriguez, R.; Chong, D.; Reibenspies, J. H.; Soriaga, M. P.; Darensbourg, M. Y. *J. Am. Chem. Soc.* **2004**, *126*, 12004–12014.

- (68) Schüth, F.; Bogdanovic, B.; Felderhoff, M. *Chem. Commun.* **2004**, 2249–2258.
 (69) Rowsell, J. L. C.; Yaghi, O. M. *Angew. Chem., Int. Ed.* **2005**, *44*, 4670–4679.
 (70) Forster, P. M.; Eckert, J.; Chang, J. S.; Park, S. E.; Ferey, G.; Cheetham, A. K. *J. Am. Chem. Soc.* **2003**, *125*, 1309–1312.
 (71) Chen, B.; Ockwig, N. W.; Millward, A. R.; Contreras, D. S.; Yaghi, O. M. *Angew. Chem., Int. Ed.* **2005**, *44*, 4745–4749.
 (72) McKeown, N. B.; Gahm, B.; Msayib, K. J.; Budd, P. M.; Tattershall, C. E.; Mahmood, K.; Tan, S.; Book, D.; Langmi, H. W.; Walton, A. *Angew. Chem., Int. Ed.* **2006**, *45*, 1804–1807.
 (73) Hu, X.; Skadtchenko, B. O.; Trudeau, M.; Antonelli, D. M. *J. Am. Chem. Soc.* **2006**, *128*, 11740–11741.
 (74) Ferey, G.; Latroche, M.; Serre, C.; Millange, F.; Loiseau, T.; Percheron-Guegan, A. *Chem. Commun.* **2003**, 2976–2977.
 (75) Basic Research Needs for the Hydrogen Economy; http://www.eere.energy.gov/hydrogenandfuelcells/pdfs/hydrogen_posture_plan.pdf, 2004.

purified using an MBraun Solvent Purification System. CD_2Cl_2 was distilled under a vacuum from CaH_2 . $\text{C}_6\text{D}_5\text{CD}_3$ was vacuum transferred from a Na mirror. $[\text{Fe}(\eta^5\text{-C}_5\text{H}_5)_2][\text{BARF}_4]$,⁴⁰ $[\text{Rh}_6(\text{PCy}_3)_6\text{H}_{12}][\text{BARF}_4]_2$ **Cy-[H12]**²⁺, and $[\text{Rh}_6(\text{P}^i\text{Pr}_3)_6\text{H}_{12}][\text{BARF}_4]_2$ **ⁱPr-[H12]**²⁺ were prepared according to the published procedures.²⁰ $\text{Cr}(\eta^6\text{-C}_6\text{H}_6)_2$, $\text{Co}(\eta^5\text{-C}_5\text{H}_5)_2$, and $[\text{Fe}(\eta^5\text{-C}_5\text{H}_5)_2][\text{PF}_6]$ were purchased from Strem and Aldrich and used as received.

NMR Spectroscopy. ¹H and ³¹P NMR spectra were recorded on a Bruker Avance 400 MHz FT-NMR spectrometer. Residual protio solvent was used as reference for ¹H NMR spectra (CD_2Cl_2 : $\delta = 5.33$, $\text{C}_6\text{D}_5\text{CD}_3$ $\delta = 2.09$). ³¹P NMR spectra were referenced against 85% H_3PO_4 (external). Coupling constants are quoted in hertz. ¹H NMR spectra were recorded using long delays between pulses (> 5 s) to avoid saturation. T_1 measurements were made using the standard inversion–recovery–delay method ($180^\circ\text{-}\tau\text{-}90^\circ$) method.

Mass Spectrometry. ESI-MS data were collected on a Waters Micromass Q-ToF micro mass spectrometer in positive ion mode. Samples were infused by means of a syringe pump at $5 \mu\text{L min}^{-1}$. Solutions were made up in an inert-atmosphere glovebox using dry CH_2Cl_2 . Capillary voltage was set to 2900 V. To minimize fragmentation of the parent ion, the cone voltage was set to 10 V and source and desolvation gas temperatures were both set to 30 °C. Theoretical isotope patterns were calculated using Matthew Monroe's Molecular Weight Calculator (<http://jjorg.chem.unc.edu/personal/monroe/mwtwin.html>).

X-ray Crystallography. Intensity data for **Cy-[H12]**⁺ were collected at 150 K on a Nonius KappaCCD diffractometer using graphite monochromated Mo K α radiation ($\lambda = 0.71073 \text{ \AA}$). Intensity data for **ⁱPr-[H12]** were recorded on a Bruker ApexII CCD diffractometer using synchrotron radiation on Station 9.8 of the SRS. Both instruments were equipped with an Oxford Cryosystems cooling device. Data for **Cy-[H12]**⁺ were processed using the supplied Nonius Software, while those for **ⁱPr-[H12]** were processed using the Bruker suite of programs APEX v2.0-2. For **Cy-[H12]**⁺ a symmetry-related (multiscan) absorption correction was employed. Crystal parameters and details on data collection, solution, and refinement for the complexes are provided in Table 2. Structure solution, followed by full-matrix least-squares refinement, was performed using the WinGX-1.70 suite of programs throughout. Crystallographic data files have been deposited with the Cambridge Crystallographic Data Service (CCDC, 12 Union Road, Cambridge CB2 1EZ (UK); Telephone: (+44) 1223-336-408, Fax: (+44) 1223-336-033, E-mail: deposit@ccdc.cam.ac.uk). **Cy-[H12]**⁺ 603 589, **ⁱPr-[H12]** 621 584.

Electrochemical Experiments. For voltammetric measurements an Autolab PGSTAT30 potentiostat system (EcoChemie, Netherlands) was employed with a Pt mesh counter electrode and a silver wire pseudo-reference electrode (calibrated versus internal ferrocene). A 3.0 mm diameter glassy carbon electrode (BASi, USA) and a 10 μm diameter platinum microdisc electrode were employed as working electrodes. Solutions in dry dichloromethane were prepared with 0.01 M $[\text{NBu}_4][\text{BARF}_4]$ and under dry argon. Ferrocene was employed as an internal reference. The Digisim software package (Digisim3, Cyclic voltammetric Simulator for Windows, Version 3.03, BASi, USA) was employed for the determination of rate constants from cyclic voltammetry data. Steady state measurements at a 10 μm diameter platinum microelectrode confirmed all processes to be one electron in nature (with a diffusion coefficient of $D = kT/6\pi\eta a = 5.8 \times 10^{-10} \text{ m}^2 \text{ s}^{-1}$ consistent with the Stokes–Einstein equation). Although the redox processes described here appear quite straightforward, we cannot discount that they mask more complex and subtle events.

EPR. For EPR analysis a sample of **Cy-[H12]**⁺ was placed into a quartz suprasil EPR tube in 1,2- $\text{C}_6\text{H}_4\text{F}_2$ solution. The X-band (9.371 GHz) EPR spectra were recorded at room temperature on a cw-Bruker EMX spectrometer operating at 100 kHz field modulation and equipped

with an ER-4119HS high-sensitivity cavity. Accurate *g* values were determined with respect to a DPPH standard.

SQUID Magnetometry. The magnetization of compound **ⁱPr-[H12]** was determined using a Quantum Design MPMS2 SQUID magnetometer. The sample was sealed in a 5 mm NMR tube and measured in applied fields of 0.1 and 1 T from 1.8 to 340 K. No significant difference was observed in the susceptibility, χ , as a function of field. Data were corrected for the diamagnetism of the constituent atoms, and the effective moment, μ_{eff} , deduced from these data using the relationship $\mu_{\text{eff}} \approx (8\chi T)^{0.5}$, where χ is expressed in units of emu.

Synthesis of $[(\text{PCy}_3)_6\text{Rh}_6\text{H}_{12}][\text{BARF}_4]$, **Cy-[H12]⁺.** $[(\text{PCy}_3)_6\text{Rh}_6\text{H}_{12}][\text{BARF}_4]_2$ **Cy-[H12]**²⁺ (20 mg, 4.9 μmol) and $(\text{C}_6\text{H}_6)_2\text{Cr}$ (2.3 mg, 11 μmol) in 1,2-difluorobenzene (2 mL) were sonicated for 5 min. The solvent was removed in vacuo, and the residue was repeatedly crystallized from fluorobenzene/toluene until minimal pale colored material crystallized. Slow diffusion of toluene into a concentrated solution of the dark solid in fluorobenzene gave $[(\text{PCy}_3)_6\text{Rh}_6\text{H}_{12}][\text{BARF}_4]$ **Cy-[H12]**⁺ as dark green crystals (12 mg, 76%). Addition of an equimolar amount of $[\text{Fe}(\eta^5\text{-C}_5\text{H}_5)_2][\text{BARF}_4]$ to a CD_2Cl_2 solution of **Cy-[H12]**⁺ returned a diamagnetic ¹H NMR spectrum showing signals assigned to **Cy-[H12]**²⁺ and an ESI-MS spectrum that also showed the formation of the dicationic cluster.

¹H NMR (400 MHz, CD_2Cl_2): δ 35.7 (br s, fwhm 430 Hz, 6H, CH), 16.5 (br s, fwhm 275 Hz, 6H, CH), 7.71 (m, 8H, BARF_4), 7.53 (s, 4H, BARF_4), 5.4 (br s, fwhm 380 Hz, 6H, CH), -2.0 to 4.9 (m, 180H, CH_2).

nb: Paramagnetic. no hydride signals observed, and no signals observed in the ³¹P{¹H} NMR spectrum. An Evans measurement³⁹ (CH_2Cl_2) gave $\mu_{\text{eff}} = 1.82$ (1 unpaired electron would have $\mu_{\text{eff}} = 1.73$).

Elemental Analysis calcd for $\text{C}_{140}\text{H}_{222}\text{B}_1\text{F}_{24}\text{P}_6\text{Rh}_6\text{C}_7\text{H}_8$: %C, 54.0; %H, 7.1. Found: %C, 53.8; %H, 7.0. (Toluene was found in the X-ray structure.) ESI-MS, $\text{Rh}_6\text{C}_{108}\text{H}_{210}\text{P}_6$ calcd 2310.9, obsd 2311.0

Hydrogen Addition to **Cy-[H12]⁺ To Give $[(\text{PCy}_3)_6\text{Rh}_6\text{H}_{14}][\text{BARF}_4]$, **Cy-[H14]**⁺.** A solution of **Cy-[H12]**⁺ (2 mg) in $\text{C}_6\text{H}_4\text{F}_2$ (5 mL) was placed under an atmosphere of hydrogen (1 atm), and the solution was allowed to stand for 16 h. A change in the UV spectrum of the solution suggested hydrogen uptake had occurred. ESI-MS, $\text{Rh}_6\text{C}_{108}\text{H}_{212}\text{P}_6$ calcd 2312.9, obsd 2313.1

$[\text{Rh}_6(\text{P}^i\text{Pr}_3)_6\text{H}_{12}]$, **ⁱPr-[H12].** $[\text{Rh}_6(\text{P}^i\text{Pr}_3)_6\text{H}_{12}][\text{BARF}_4]_2$ (10 mg, 2.90 μmol) and $(\eta^5\text{-C}_5\text{H}_5)_2\text{Co}$ (2.5 mg, 13 μmol) in difluorobenzene (3 mL) were shaken for 10 min. The mixture was slowly concentrated to dryness in vacuo, and the residue was (partially) dissolved in pentanes (5 mL). The solution was filtered, the filtrate was concentrated to ca. 2 mL in vacuo, and the solution was held at -20°C overnight to give the product as dark green-blue crystals of $[\text{Rh}_6(\text{P}^i\text{Pr}_3)_6\text{H}_{12}]$ **ⁱPr-[H12]** (2.5 mg, 54%). Elemental Analysis $\text{C}_{54}\text{H}_{138}\text{Rh}_6\text{P}_6$ requires: %C, 40.8; %H, 8.7. Found: %C, 41.1; %H, 8.7

¹H NMR (400 MHz, $\text{C}_6\text{D}_5\text{CD}_3$): δ 30.87 (s, 18H, fwhm 83 Hz, PCH), 0.59 (s, 108H, CH_3).

nb: Paramagnetic. no hydride signals observed, and no signals observed in ³¹P{¹H} NMR spectrum. An Evans measurement³⁹ (toluene) gave $\mu_{\text{eff}} = 2.89$ (two unpaired electrons would have $\mu_{\text{eff}} = 2.83$).

$[\text{Rh}_6(\text{P}^i\text{Pr}_3)_6\text{H}_{14}]$ **ⁱPr-[H14].** A solution of **ⁱPr-[H12]** in $\text{C}_6\text{D}_5\text{CD}_3$, in a J. Youngs NMR tube, was frozen in liquid nitrogen, placed under 1 atm of hydrogen, sealed, and allowed to warm to room temperature ($298/77 \approx 4$ atm). The solution was allowed to stand for 16 h, and the product was characterized in situ by ¹H and ³¹P NMR spectroscopy.

¹H NMR (400 MHz, $\text{C}_6\text{D}_5\text{CD}_3$, 298 K): δ 2.19 (apparent octet, splitting 7.2 Hz, 18H, PCH), 1.19 (virtual quartet, splitting 6.7 Hz, 108H, CH_3), -25.60 (br s, $\sim 13\text{H}$, Rh–H).

³¹P{¹H} NMR (162 MHz, $\text{C}_6\text{D}_5\text{CD}_3$): δ 97.05 (br s, fwhm 530 Hz).

Selected ¹H NMR (400 MHz, $\text{C}_6\text{H}_5\text{CD}_3$, 250 K): δ -24.90 (s br, $T_1 = 72$ ms), -25.82 (s br, $T_1 = 72$ ms). Ratio of these two peaks is

1:2.5. $^{31}\text{P}\{^1\text{H}\}$ NMR (162 MHz, $\text{C}_6\text{H}_5\text{CD}_3$): δ 99.1 [d, $J(\text{Rh}-\text{P})$ 195 Hz], 87.5 [d, $J(\text{Rh}-\text{P})$ 153 Hz]. Ratio of these two peaks is 2.5:1.

Acknowledgment. We thank the Royal Society (University Research Fellowship to A.S.W.) and the EPSRC (GR/T10169) for funding. Dr. Damien Murphy is thanked for the ESR measurements. Professor Jennifer Green and Dr. Nilay Hazari are thanked for insightful comments on the manuscript and stimulating discussions. Dedicated to Professor Thomas Fehlner on the occasion of his retirement.

Supporting Information Available: Cyclic voltamograms of $^i\text{Pr}-[\text{H12}]^{2+}$, $\text{Cy}-[\text{H12}]^{2+}$ on a platinum counter electrode and $\text{Cy}-[\text{H16}]^{2+}$ under 1 atm of H_2 . Electronic absorption spectra for solutions of $\text{Cy}-[\text{H12}]^{2+}/\text{Cy}-[\text{H16}]^{2+}$; $\text{Cy}-[\text{H12}]^+/\text{Cy}-[\text{H14}]^+$; $^i\text{Pr}-[\text{H12}]/^i\text{Pr}-[\text{H14}]$. CIF files for all the crystal structures reported in this paper. This material is available free of charge via the Internet at <http://pubs.acs.org>.

JA066940M